Heliyon 10 (2024) e23808

Contents lists available at ScienceDirect

Heliyon

journal homepage: www.cell.com/heliyon

Access to carbonyl compounds *via* the electroreduction of *N*-benzyloxyphthalimides: Mechanism confirmation and preparative applications

Diego Francisco Chicas-Baños [a,b,*], Mariely López-Rivas [c], Felipe J. González-Bravo [d], Fernando Sartillo-Piscil [e], Bernardo Antonio Frontana-Uribe [b,c,**]

[a] *Universidad de El Salvador (UES), Facultad de Ciencias Naturales y Matemática, Escuela de Química, Final 25 Av. Nte, 1101, San Salvador, El Salvador*
[b] *Universidad Nacional Autónoma de México, Instituto de Química, Ciudad Universitaria, Mexico City, 04510, Mexico*
[c] *Centro Conjunto Química Sustentable UAEMéx-UNAM, Km 14.5 Carretera Toluca-Ixtlahuaca, Toluca, 50200, Estado de México, Mexico*
[d] *Departamento de Química, Centro de Investigación y Estudios Avanzados, Av. Instituto Politécnico Nacional 2508, 07360, Mexico City, Mexico*
[e] *Centro de Investigación de la Facultad de Ciencias Químicas, Benemérita Universidad Autónoma de Puebla (BUAP), 14 Sur Esq. San Claudio, Col. San Manuel, 72570, Puebla, Mexico*

ARTICLE INFO

Keywords:
Organic electrosynthesis
Electrochemical catalysis
Aldehyde synthesis
Cyclic voltammetry simulations

ABSTRACT

A method to access carbonyl compounds using reductive conditions was evaluated *via* electrochemical reduction of their corresponding *N*-benzyloxyphthalimide derivatives (NBOPIs). The mechanism of this originally reported electrochemical reaction was proposed based on DFT calculation and is experimentally confirmed herein, contrasting simulated and experimental cyclic voltammetry data. The reaction scope studied in a preparative scale and using redox sensitive functional groups showed good selectivity and tolerance toward oxidation under the reaction conditions with a moderate to good yield (50–71%). Nevertheless, some restrictions with reducible functional groups, like benzyl-brominated and nitro-aromatic derivatives, were observed. The present approach can be considered a self-sustainable electrochemical catalysis for the synthesis of aromatic carbonylic compounds passing through anion radical intermediates produced by a cathodic reaction.

1. Introduction

Although a large variety of efficient approaches exist for transforming benzyl alcohols to their corresponding carbonyl derivatives, only a few follow the green chemistry principles [1–5]. Accordingly, chemists are always looking for suitable mild reaction conditions that could be selectively applied on substrates that contain further oxidizable moieties, avoiding protecting groups. In this way, the synthetic route design should avoid protection-deprotection protocols.

Due to the intrinsic properties of the heterogeneous electron transfer reactions, one of the basics of electrochemical synthesis, it is an excellent choice for developing environmentally friendly oxidation and reduction reactions according to the green chemistry spirit

* Corresponding authorUniversidad de El Salvador (UES), Facultad de Ciencias Naturales y Matemática, Escuela de Química, Final 25 Av. Nte, 1101, San Salvador, El Salvador
** Corresponding authorUniversidad Nacional Autónoma de México, Instituto de Química, Ciudad Universitaria, Mexico City, 04510, Mexico
E-mail addresses: diego.chicas@ues.edu.sv (D.F. Chicas-Baños), bafrontu@unam.mx (B.A. Frontana-Uribe).

https://doi.org/10.1016/j.heliyon.2023.e23808
Received 7 August 2023; Received in revised form 10 December 2023; Accepted 13 December 2023
Available online 21 December 2023

[6]. Electrogeneration of reactive intermediates, like radical ions and free radicals, provides widespread opportunities for designing new organic reactions [7–10].

Since Kim's publication regarding the generation of *O*- and *C*-centered radicals from *N*-alkoxyphthalimides (NAPIs) using organotin reagents (Scheme 1a) [11], various remarkable synthetic strategies have been reported. For example, Sammis published the versatility of the alkoxy radicals in the intramolecular radical addition to olefins [12–15]. Additionally, other groups have reported the use of alkoxyl radicals photochemically produced in either the total synthesis of natural products or the synthesis of relevant *O*-heterocyclic compounds [16–20]. Nevertheless, the reactivity of *N*-benzyloxyphthalimides (NBOPIs) is quite different. Sammis and coworkers studied the behavior of this family of substrates through a photoredox reaction (Scheme 1b) [21], finding that the fragmentation of the NBOPI radical anion to carbonyl compounds is a highly favorable process. To rationalize this observation, a concerted intramolecular fragmentation process (Scheme 1c) was proposed. Likewise, the electrochemical behavior of NBOPIs at only the electroanalytical level was reported by Terent'ev and coworkers (Scheme 1b), describing similar reactivity to the photochemical reaction [22]. The final carbonyl products were identified using cyclic voltammetry (CV) without any other information because the objective of the authors was not a synthetic approach. Therefore, neither preparative reaction was attempted nor isolated yields of the aldehydes obtained were reported [22]. Based on DFT calculations, the latter authors proposed a mechanism that until now has not been experimentally validated. Due to the role of phthalimide in the reaction, the authors described this reaction as a "self-sustaining catalysis" (n < 1 e, Scheme 1d).

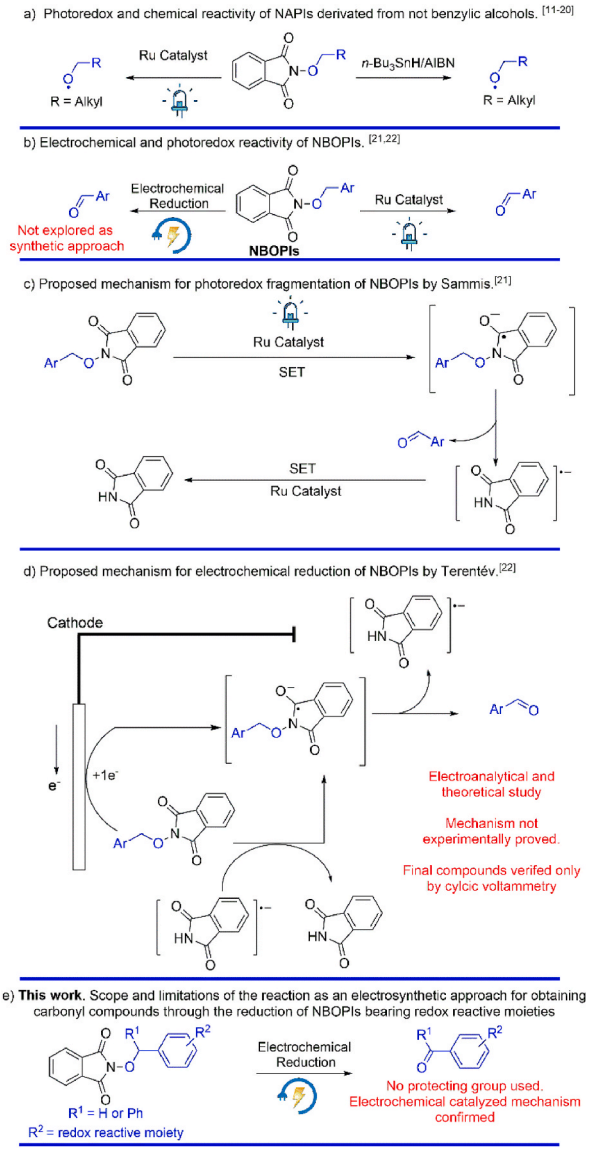

Scheme 1. Reactivity of NAPIs and NBOPIs, chemically, photoredox catalyzed, and electrochemically induced.

Encouraged by these exciting findings and motivated by the synthetic potential and the electro-organic applications of this reaction, the development of a synthetic methodology that enables the access to carbonyl compounds containing other redox reactive moieties, *via* the electroreduction of the corresponding NBOPIs derivatives (Scheme 1e), was envisioned. In addition, cyclic voltammetry simulations of the proposed mechanism and its comparison with the experimental CV behavior were used to revise and validate the originally proposed reaction mechanism reported [22], which can be simplified as an EC_1C_2 mechanism (Scheme 2) [23].

2. Experimental

2.1. General considerations

Commercially purchased reagents were used as starting materials without any additional purification steps. The supporting electrolyte salts were dried in the oven for at least one night before use. Anhydrous-grade solvents were used for both Mitsunobu reactions, preparative electrolysis, and cyclic voltammetry experiments. For purification by column chromatography (CC), silica gel (70–230 mesh) and technical grade solvents but previously distilled were used. TLC analysis was carried out using Merck TLC Silica gel 80 F254 aluminum sheets.

2.2. Synthesis of NBOPIs

The following methods for NBOPIs' synthesis were adapted from previous reports [24–27]:

Method A: In a 35-mL vial for Discover SP microwave reactor, 3.3 mmol of DIAD or DEAD were dissolved in 10 mL of anhydrous tetrahydrofuran (THF), and 3.3 mmol of triphenylphosphine (TPP) were added under continuous agitation in an ice-bath. Then, 3.0 mmol of *N*-hydroxyphthalimide (NHPI) and 3.0 mmol of the corresponding benzylic alcohol were dissolved in 10.0 mL of THF and added to the microwave reactor to immediately carry out the microwave program for the synthesis. The solvent was removed from the reaction crude using rotary evaporation, and the residue was supported on silica gel to be separated using flash column chromatography with a mixture of *n*-hexane and ethyl acetate as eluent. Method B: In a 100-mL round bottom flask, 3.3 mmol of DIAD or DEAD were dissolved in 10 mL of anhydrous tetrahydrofuran (THF), and 3.3 mmol of triphenylphosphine (TPP) were added under continuous agitation in an ice-bath. Then, 3.0 mmol of (NHPI) and 3.0 mmol of the corresponding benzyl alcohol were dissolved in 10.0 mL of THF and added to the microwave reactor to continue agitation until the reaction was finished (usually 30–60 min). The solvent was removed using rotary evaporation and the residue was supported on silica gel to be separated using flash column chromatography with a mixture of *n*-hexane and ethyl acetate as eluent. Method C: In a 100 mL round bottom flask, 3.0 mmol of NHPI and the corresponding benzyl bromide (3 mmol) were dissolved in 20 mL of DMF. Using a dropping funnel, 3.0 mmol of DBU dissolved in 5 mL of DMF were added, drop by drop, to the flask and sonicated for 3–5 h until the reaction was finished. Then, an aqueous solution of

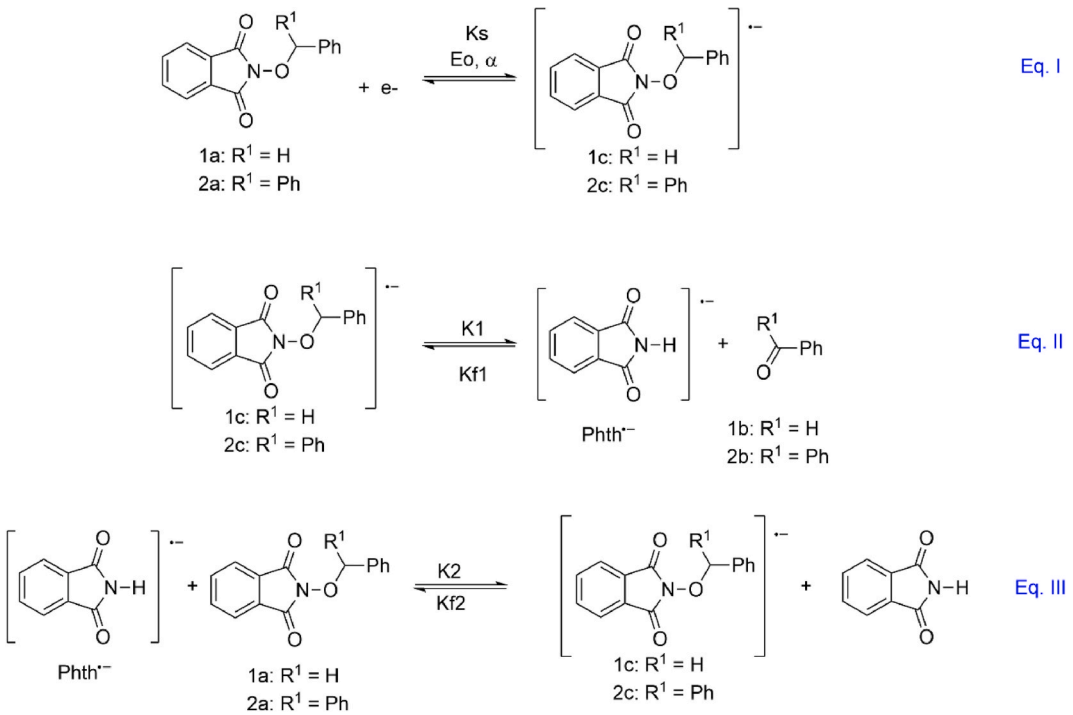

Scheme 2. EC_1C_2 mechanism used to simulate the experimental voltammograms for the electrochemical reduction of **1a** and **2a**.

HCl (10%) was added until neutralization. The insoluble product was filtered and purified using recrystallization or flash column chromatography with a mixture of *n*-hexane and ethyl acetate as eluent.

2.3. Electroanalytical experiments to confirm the mechanism

Cyclic voltammetry (CV) studies were carried out using an Autolab PGSTAT30 controlled by the NOVA 2.1 software, applying positive feedback resistance compensation (385 Ω), using an electrochemical cell containing 10 mL solution of 0.1 M of tetrabutylammonium perchlorate ($TBAClO_4$) in DMF.

Before the beginning of each experimental run, this solution was purged with N_2 for 10 min. A glassy carbon electrode and a platinum wire were used as working and counter electrodes, respectively. The reference electrode was prepared with a silver wire in a solution of 0.1 M $TBAClO_4$, 0.01 M $AgNO_3$ in acetonitrile. The scan rate study was carried out using a 5 mM solution of **1a** and **2a**. The voltammetric responses at 0.1–1.0 V/s were evaluated. In addition, the effect of the concentration of **2a** (1 mM, 2 mM, 5 mM, and 10 mM) on the voltammetric behavior was performed at 0.1 V/s.

2.4. Simulation of the experimental voltammograms

The reaction mechanism depicted in Scheme 2 was used to carry out the simulation tests using the software Digisim 3.03 from Bioanalytical Systems Inc, West Lafayette USA. ® The reaction sequence was introduced into the software, changing the different thermodynamic and kinetic reaction parameters until the simulated CVs fitted with the experimental ones. In general, the reaction may be described as an EC_1C_2 mechanism, where C_2 is a father-son process (Eq. III in Scheme 2). The CVs of phthalimide and the released carbonyl product were also simulated to describe the complete experimental voltammograms of NBOPIs on the larger scale of electrode potential.

2.5. Electrosynthesis setup

The electrosynthesis experiments were carried out in two stages: (1) preparative electrolysis experiments to screen conditions for the synthesis of the carbonyl compounds, and (2) the application of the best conditions found to explore the scope of the reaction. The screening experiments were carried out in the ElectraSync 2.0 equipped with the carrousel device for multiple electrolysis. All the reactions were set in a controlled current mode, using carbon electrodes (graphite), varying the solvent, supporting electrolyte, and current density. As general conditions, 8 mL of a 0.1 M solution of the supporting electrolyte was used ($TBAPF_6$, $TBAClO_4$, and $LiClO_4$). Before beginning the electrolysis, this solution was purged with N_2 for 10 min **2a** prepared from benzhydrol (0.5 mmol) was selected to evaluate the corresponding generation of benzophenone (**2b**) and the yield was evaluated using GC-FID.

The scope and limitation of the reaction were evaluated using the ElectraSync 2.0 device and accessories or the four-channel R&S®HMP4000 power supply, applying the best conditions found for benzophenone electrosynthesis. Both carbon electrodes, 3.33 mA/cm^2 in a solution of 0.1 M $TBAPF_6$ and 0.1 M of the substrate in anhydrous acetonitrile were used. The reaction progress was monitored using TLC and stopped when the starting material was consumed or after passing a maximum of 1.5 F/mol of charge. The solvent was removed from the reaction's crude using rotary evaporation and supported on silica gel to be separated using flash column chromatography with a mixture of *n*-hexane and ethyl acetate as eluent. The yields of the reactions were also evaluated using NMR spectroscopy in the reaction's crude using benzhydrol as an internal standard.

2.6. Spectroscopy and characterization of the NBOPIS

2-(benzyloxy)isoindoline-1,3-dione (1a): [28] white solid, m. p.142–143 °C;^{1}H NMR (300 MHz, $CDCl_3$): δ = 7.70 (4H, dm), 7.47 (2H,m), 7.31 (3H, m), δ_H 5.14 (2H, s); ^{13}C NMR (300 MHz, $CDCl_3$): δ = 163.96, 134.92, 134.20, 130.37, 129.82, 129.35, 129.03, 123.96, 80.35.

2-(benzhydryloxy)isoindoline-1,3-dione (2a): [29] white solid, m. p.159–160 °C; ^{1}H NMR (300 MHz, $CDCl_3$): δ = 7.63 (4H, dm), 7.47 (4H, dd), 7.27 (6H, m), 6.46 (1H, s); ^{13}C NMR (300 MHz, $CDCl_3$): δ 163.71, 137.89, 134.35, 128.87, 128.76, 128.60, 128.52, 128.40, 128.35, 123.40, 89.66.

2-((3-(bromomethyl)benzyl)oxy)isoindoline-1,3-dione (3a): white solid, m. p.119–120 °C; ^{1}H NMR (300 MHz, $CDCl_3$): δ: 7.77 (4H,dm), 7.56 (1H, t), 7.48 (1H, dt), 7.39 (2H, m), 5.20 (2H, s), 4.49 (2H,s); ^{13}C NMR (300 MHz, $CDCl_3$) δ 163.47, 138.24, 134.55, 134.43, 130.39, 130.03, 129.86, 129.15, 128.87, 123.58, 79.43, 33.03, HRMS (ESI): *m/z* calcd for $C_{16}H_{12}BrNO_3$+H^+: 346.00788 $[M+H]^+$; found: 346.00912.

2-((2-(bromomethyl)benzyl)oxy)isoindoline-1,3-dione (4a): [30] cream solid, m. p. 133–134 °C; ^{1}H NMR (300 MHz, $CDCl_3$): δ = 7.78 (4H,dm), 7.44 (1H, d), 7.41 (1H, td), 7.30 (H, td), 5.37 (2H, s), 4.99 (2H,s); ^{13}C NMR (300 MHz, $CDCl_3$): δ = 163.50, 138.63, 134.57, 132.27, 132.03, 130.95, 130.41, 128.91, 128.82, 123.60, 77.14, 30.98.

2-((3-(hydroxymethyl)benzyl)oxy)isoindoline-1,3-dione (5a): white solid, m. p.144–146 °C; 1H NMR (300 MHz, $(CD_3)_2CO$/DMSO-D_6): δ = 7.85 (4H,dm), 7.55 (1H, s), 7.39 (3H, m), 5.21 (2H, s), 4.66 (2H, s), 4.38 (1H,br); ^{13}C NMR (300 MHz, $CDCl_3$): δ = 164.44, 144.49, 135.95, 135.52, 130.40, 129.52, 129.31, 129.08, 128.50, 124.40, 80.86, 64.58. HRMS (ESI): *m/z* calcd for $C_{16}H_{13}NO_4$+H^+: 284.09228 $[M+H]^+$; found: 284.09250.

2-((4-(hydroxymethyl)benzyl)oxy)isoindoline-1,3-dione (6a): white solid, m. p.157–159 °C; ^{1}HNMR (300 MHz, $CDCl_3$/DMSO-D_6): δ = 7.77 (4H,m), 7.36(4H, M), 7.39 (3H, m), 5.09 (2H, s), 4.85 (1H, br), 4.54 (2H,d); ^{13}C NMR (300 MHz, $CDCl_3$/DMSO-D_6): δ =

168.13, 148.32, 139.41, 137.03, 134.56, 133.48, 131.51, 128.21, 84.39, 68.47. HRMS (ESI): *m/z* calcd for $C_{16}H_{13}NO_4$+NH_4^+: 301.11883 $[M + NH_4]^+$; found: 301.11857.

2-((4-methoxybenzyl)oxy)isoindoline-1,3-dione (7a): [31] white solid, m. p.135–136 °C; ^{1}HNMR (300 MHz, $CDCl_3$) δ = 7.65 (4H, 2 m), 7.35(2H, d), 6.77 (2H, d), 5.05 (2H, s), 3.69 (3H, t); ^{13}C NMR (300 MHz, $CDCl_3$) δ = 163.59, 160.48, 134.44, 131.69, 128.93, 125.90, 123.48, 113.96, 79.53, 55.29.

2-((4-hydroxybenzyl)oxy)isoindoline-1,3-dione (8a): [27] white solid, m. p.185–188 °C; ^{1}HNMR (300 MHz, CDCl3/DMSO-D6) δ = 9.35 (1H, t, br), 7.74(4H, m), 7.23 (2H, m), 6.71 (2H, m), 4.97 (2H, d); ^{13}CNMR (300 MHz, $CDCl_3$/DMSO-D_6) δ = 162.89, 158.06, 134.10, 131.20, 128.25, 123.73, 122.87, 115.03, 79.16.

2-((4-nitrobenzyl)oxy)isoindoline-1,3-dione (9a): [32] green solid, m. p.196–197 °C; ^{1}HNMR (300 MHz, $CDCl_3$) δ = 8.12 (2H, d), 7.73(6H, m), 5.26 (2H, s). ^{13}CNMR (300 MHz, $CDCl_3$/DMSO-D_6) δ = 163.31, 148.82, 140.90, 134.75, 130.0, 128.66, 123.75, 123.73, 78.29.

Benzaldehyde (1b): [33] yellow oil, ^{1}H NMR (300 MHz, $CDCl_3$): δ = 9.99 (1H, s), 7.80 (2H, m), 7.55 (1H, t), 7.47 (2H, t).

Benzophenone (2b): [33] white solid, ^{1}H NMR (300 MHz, $CDCl_3$): δ = 7.78 (4H, m), 7.54 (2H, m), 7.81 (2H, dt), 7.43 (4H, m).

3-(Bromomethyl)benzaldehyde (3b): [34] yellow oil, ^{1}H NMR (300 MHz, $CDCl_3$): δ = 10.02 (1H, s), 7.80 (1H, ddd), 7.81 (1H, dt), 7.65 (1H, dt), 7.53 (1H, t), 4.80 (2H, s).

2-[[2-[(1,3-Dihydro-1,3-dioxo-2H-isoindol-2-yl)methyl] phenyl] methoxy] -1H-isoindole-1,3(2H)-dione (4c): white solid, ^{1}H NMR (300 MHz, $CDCl_3$): δ = 7.74 (4H, m), 7.63 (4H, m), 7.42 (1H, d), 7.27 (2H, m), 7.15 (1H, td), 5.52 (2H, s), 5.22 (2H, s),^{13}C NMR (75 MHz, $CDCl_3$) δ = 167.96, 163.18, 137.28, 134.10, 133.67, 131.83, 131.48, 129.94, 129.55, 128.59, 127.56, 123.20, 123.02, 77.59, 37.85. HRMS (ESI): *m/z* calcd for $C_{24}H_{16}N_2O_5$+H^+: 413.11375 $[M+H]^+$; found: 413.11322.

3-(Hydroxymethyl)benzaldehyde (5b): [35] white solid, m. p.116–118 °C; ^{1}H NMR (300 MHz, $CDCl_3$): δ = 9.97 (1H, s), 7.85 (1H, s), 7.77 (1H, d), 7.67(1H, d), 7.49 (1H, t), 4.75 (2H, s), 2.61 (1H, br).

4-(Hydroxymethyl)benzaldehyde (6b): [36] colorless oil, ^{1}H NMR (300 MHz, $CDCl_3$): δ = 9.99 (1H, s), 7.87 (2H, d), 7.50 (2H, d), 7.67(2H, s), 2.19 (1H, br).

4-Methoxybenzaldehyde (7b): [33] colorless oil, ^{1}H NMR (300 MHz, $CDCl_3$): δ = 9.80 (1H, s), 7.75 (2H, dt), 6.92 (2H, dt), 3.80 (3H, s).

4-Hidroxybenzaldehyde (8b): [37] white solid, m. p. 120–122 °C, ^{1}H NMR (300 MHz, $CDCl_3$/DMSO-D_6): δ = 10.43 (1H, br), 10.18 (1H, s), 8.12 (2H, d), 7.33 (2H, d).

3. Results and discussion

3.1. Mechanistic studies and CV simulations

A previous report widely discussed whether an *O*- centered or an *N*-centered radical is formed during the *N–O* scission of the radical anion formed (**1c**) during the reduction of **1a** [22]. Based on DFT calculations, these authors found that during the scission of the *N–O* bond, the alkoxy radical is more likely to be formed instead of the *N*-radical, which eventually leads to the carbonyl compound **1b** (Scheme 3).

To experimentally confirm the mechanism proposed in Scheme 2, the comparison between the simulated and experimental CVs of **2a** was carried out (Fig. 1). Accordingly, benzophenone (**2b**) and phthalimide (**PhtH**) are the cathodic reduction products (Scheme 4). As can be observed, mechanism of Scheme 2 is a simplification of the complete mechanism shown in Scheme 3, and equation 2 is a

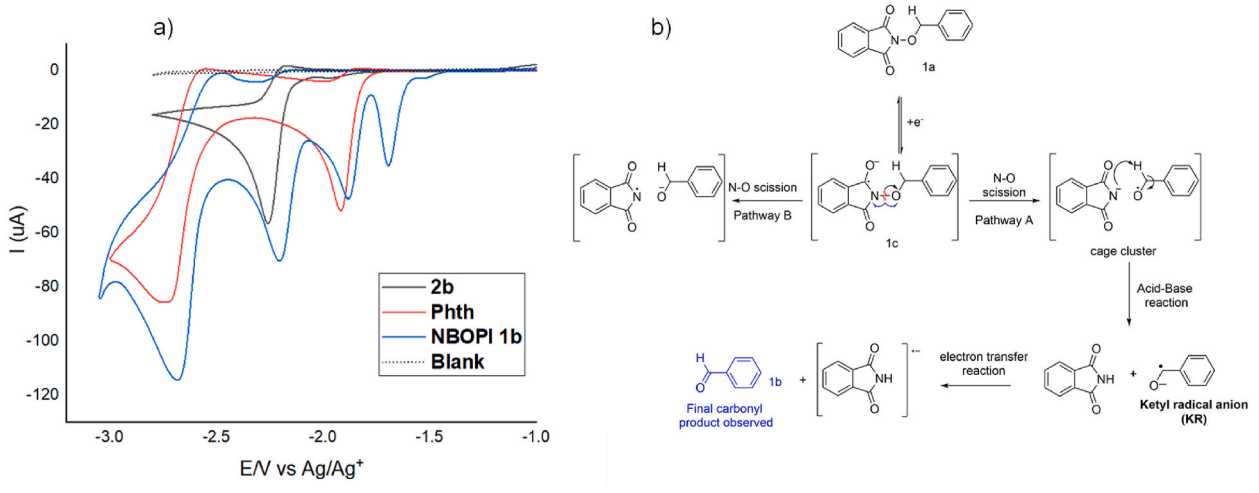

Scheme 3. (a) Cyclic voltammetry of **1a** (5 mM), benzaldehyde (5 mM) and phthalimide (5 mM), 0.1 M $TBAClO_4$ in DMF, at 0.1 V s^{-1}. WE: Glassy carbon, CE: Pt, RE: Ag/Ag^+. IR_{drop} = 95%. (b) Complete electrochemical decomposition pathway of NBOPIs proposed by Terent'ev [22].

simplification containing three rapid simple steps: the homolytic *N*–O scission, an acid-base reaction, and the electron transfer between the last two species; it was considered that the three reactions occur rapidly.

Fig. 1 shows the CV behavior of NBOPI **2a** on a wide potential scale (blue line). This voltammetric pattern is compared with the voltammograms of benzophenone (**2b**) and phthalimide (**PhtH**). The peak $\mathbf{i_c}$ corresponds to the reduction of **2a.**

The chemical nature of the species corresponding to peaks **iic**, $\mathbf{iii_c}$-$\mathbf{iii_a}$, and $\mathbf{iv_c}$-$\mathbf{iv_a}$ was inferred from the voltammetric behavior of pure samples of phthalimide ($\mathbf{ii_c}$ and $\mathbf{iv_c}$-$\mathbf{iv_a}$) and benzophenone ($\mathbf{iii_c}$-$\mathbf{iii_a}$). Benzophenone is a reversible one-electron redox system in anhydrous conditions ($\mathbf{iii_c}$-$\mathbf{iii_a}$), thus, it is the cathodic peak that can be used to calibrate the electron transfer of **2a**. The quotient of currents for **2a** and benzophenone is lower than 1, which supports the intervention of the self-consumption of **2a** in equation III of Scheme 2. In this framework, the simulation of the experimental features of the voltammogram of **2a** requires a preliminary simulation of the voltammograms of benzophenone and phthalimide.

Fig. 2 shows the voltammetric behavior of benzophenone at different scan rates (continuous lines). This compound is reduced following a simple quasi-reversible one-electron transfer process, as deduced from the peak-to-peak separation ($\Delta Ep > 56.7$ mV at 25 °C). These experimental voltammograms were simulated and the agreement with the simulated curves (dotted lines) was highly satisfactory, which means that the parameters used for this step (see Table S1, supplementary data) can be used for the subsequent simulation of NBOPI **2a** electroreduction. In the case of phthalimide, the voltammetric behavior shows a partially reversible pattern, which is typical of the intervention of a slow coupled chemical reaction following the electron transfer activation step (Fig. 3). The reduction mechanism for this compound was theoretically analyzed by Amatore and coworkers [38], and it corresponds to a self-protonation process with a fractional electronic stoichiometry (2/3). Nevertheless, herein the full voltammetric behavior at different scan rates is reported for the first time, and the mechanism and the thermodynamic and kinetic data used for simulation are in supplementary data (Table S2). Even though this reaction mechanism is more complex than that of benzophenone, the parameters used for the simulation generated an excellent fitting of the simulated voltammograms with the experimental ones.

Considering both reduction mechanisms of benzophenone and phthalimide and their kinetic and thermodynamic parameters obtained from previous simulations, a full description through the simulation of the mechanism of NBOPI **2a** electroreduction can be calculated now.

To simplify the procedure, the simulation was first performed for the first reduction peak of **2a** (Fig. 4a) and later including a wider potential scale, where the corresponding peaks of phthalimide and benzophenone were included (Fig. 4b). The experimental and simulated voltammograms of both anodic and cathodic first peaks of **2a** at different scan rates showed good fitting. The parameters that were applied for the extended mechanism simulation, which includes the electrochemical behavior of **2b** and **Phth,** are compiled in the supplementary data (Table S3). The CV simulation of **2a** in the cathodic scan agrees with the proposal of Terent'ev, where benzophenone and phthalimide are formed during the electroreduction; the mechanism also agrees with the EC_1C_2 process proposed in Scheme 2 for **2a**. Nevertheless, despite the good fitting of the cathodic peaks, the anodic peaks are not well reproduced, which makes sense because, during the scan towards the highest electrode potentials, powerful reducing species like benzophenone and phthalimide radical anions are formed. These species are therefore able to disturb all the mechanism simulated patterns after the inversion potential. Hence, the cathodic matching of the CV curve is strong evidence to confirm the mechanism proposed by Terent'ev, simulated herein and depicted in Scheme 2. Thus, it can be affirmed that NBOPIs electrochemical reduction forms the corresponding radical anion (Eq. I), which undergoes decomposition forming the desired carbonyl compound and a reduced phthalimide radical anion (Eq II). The last can trigger the starting material reduction (Eq. III) because it has a higher reduction potential ($E^\circ = -1.87$ V for phthalimide vs. $E = -1.69$ V for **2a**), generating an extra-reducing pathway that diminishes the total charge per mole used, increasing the Faradaic efficiency during the electrochemical reaction.

According to Francke and Little, this kind of mechanism can be classified as an "electrochemical catalysis" due to the fulfillment of

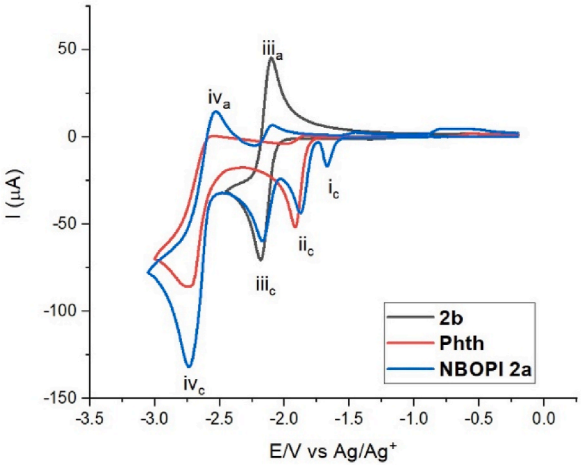

Fig. 1. Cyclic voltammetry of **2a** (5 mM), benzophenone (5 mM), and phthalimide (5 mM); 0.1 M $TBAClO_4$ in DMF, at 0.1 V s^{-1}. WE: Glassy carbon, CE: Pt, RE: Ag/Ag^+. $IR_{drop} = 95\%$.

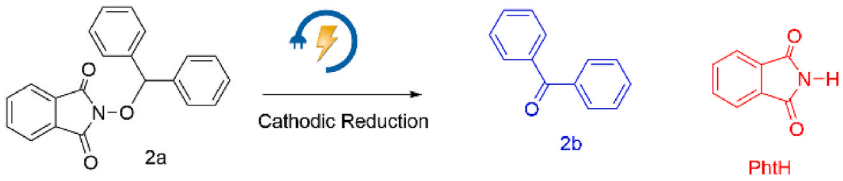

Scheme 4. Electrochemical reduction of **2a**.

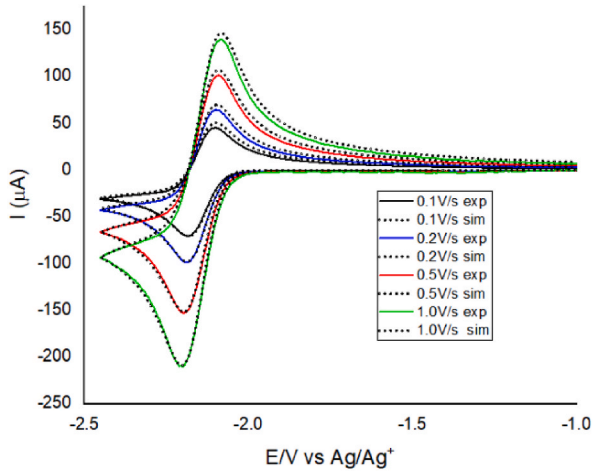

Fig. 2. Comparison between simulated (dotted lines) and experimental CV (continuous lines) for benzophenone (5 mM) at different scan rates 0.1 M $TBAClO_4$ in DMF, at 0.1 V s^{-1}. WE: Glassy carbon, CE: Pt, RE: Ag/Ag^+. IR_{drop} = 95%.

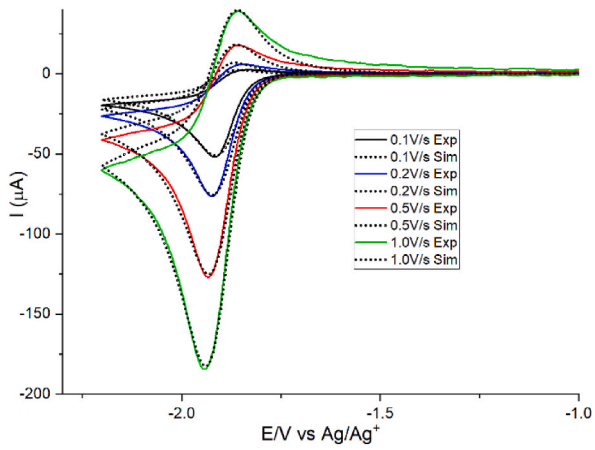

Fig. 3. Comparison between simulated (dotted lines) and experimental CV (continuous lines) for 5 mM phthalimide, at different scan rates 0.1 M $TBAClO_4$ in DMF, at 0.1 V s^{-1}. WE: Glassy carbon, CE: Pt, RE: Ag/Ag^+. IR_{drop} = 95%.

the following four requirements [39]:

1. The catalytic reduction of the reduced phthalimide (**PhtH**$^{\bullet-}$) to the starting NBOPI is thermodynamically favored due to the suitable potential difference (E**2a** < E**PhtH**$^{\bullet-}$).
2. The Brønsted basic character of the generated radical anion does not prevent triggering the chain reaction. In contrast, the radical anion undergoes *N–O* scission, yielding the alkoxy radical and the phthalimidure anion. The basicity of the anion formed allowed obtaining the desired carbonyl product (Scheme 3).
3. In the case of **1a** and **2a**, no addition or substitution reaction is feasible.
4. Finally, the data obtained for the simulation confirm that there is no reason to propose that the chain reaction is being suppressed by radical reaction as recombination or HAT (in the case of **1a** and **2a**).

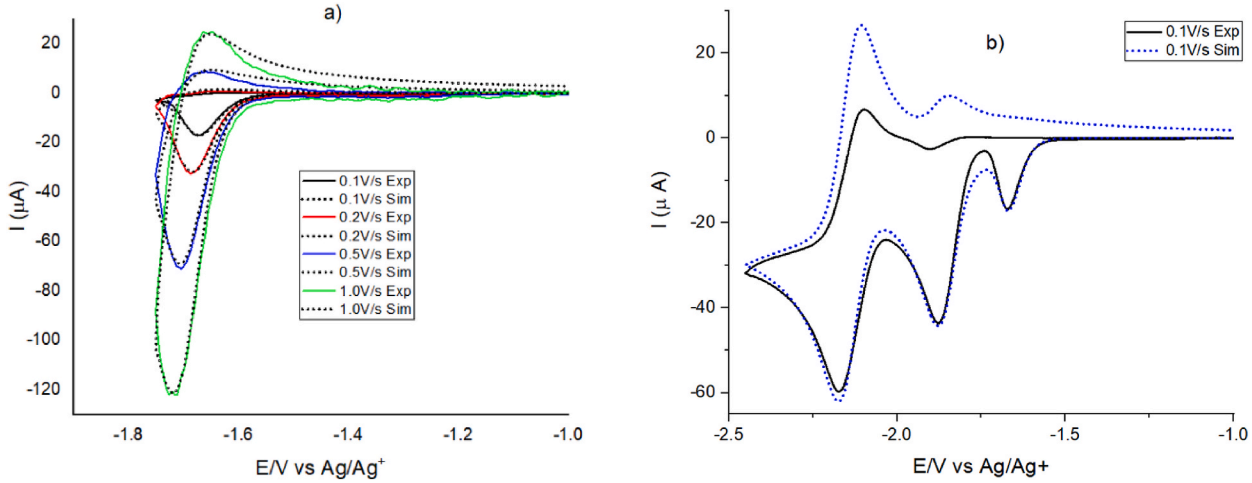

Fig. 4. Cyclic voltammetry of **2a**, 0.1 M $TBANClO_4$ in DMF, at 0.1 V s^{-1}. WE: Glassy carbon, CE: Pt, RE: Ag/Ag^+. (a) Comparison between simulated and experimental CV of the first reduction peak of **2a** at different scan rates. (b) Simulated and experimental CV of **2a.** $Ru_{drop} = 95$.

Due to the scarcity in the literature on this kind of mechanism, it can be considered appropriate to establish that the cathodic reduction of NBOPIs is an example of a formally named "electrochemical catalyzed reaction", even if the Terent'ev group named it self-sustainable electrochemical reaction [22].

3.2. Preparative electrolysis experiments

Once the mechanism of the carbonyl formation through the NBOPIs reduction was clarified, the electrosynthetic potential of this reaction for preparative transformations was evaluated. The compound **2a** was selected for screening reaction conditions, changing solvent, supporting electrolyte, and current density in a non-divided cell (Table 1). The maximum amount of charge (1.5 F/mol) was selected in function of the previous electroanalytical experiments, and the reaction's advance was monitored using TLC. The best yield of **2b** was obtained in entry 9, but it was decided not to use perchlorate salts to prevent the possibility of an explosion when perchlorates are overheated in organic media, nor DMF due to the normal workup complications and toxicity associated with this solvent. Thus, the conditions of entry 2 (Table 1) which gave 72% yield were selected to carry out the synthetic experiments for exploring the

Table 1
Screening condition for optimization reaction.

fx1

Entry	Supporting Electrolyte	J (mA/cm^2)	Charge (F/mol)	Solvent	Yield of 2b[a]
1	$LiClO_4$	3.33	1.5	MeCN	17.8
2	$TBAPF_6$	3.33	0.8	MeCN	72.0
3	$LiClO_4$	10	1.5	MeCN	17.1
4	$TBAPF_6$	10	1.5	MeCN	61.4
5	$LiClO_4$	6.67	1.5	DMF	55.7
6	$TBAPF_6$	6.67	1.5	DMF	28.7
7[b]	$LiClO_4$	6.67 (1.67)[g]	1.5	THF	25.7
8[c]	$TBAPF_6$	6.67 (3)[g]	1.5	THF	45.2
9	$TBAClO_4$	3.33	0.8	DMF	78.6
10	$TBAClO_4$	10	1.5	DMF	27.9
11[c]	$TBAClO_4$	10 (3)[g]	1.5	THF	53.6
12	$TBAClO_4$	6.67	1.0	MeCN	70.5
13	$TBAPF_6$	3.33	1.0	THF-MeCN (70–30)	57.0
14	$TBAPF_6$	6.67	1.0	THF-MeCN (70–30)	60.4
15[d]	$TBAPF_6$	3.33	0.8	MeCN	68.8
16[e,f]	$TBAPF_6$	−1.70 V	0.6	MeCN	60.0

[a] Yield determined from crude of reaction using GC-FID.
[b] Current density up to 1.67 mA/cm^2.
[c] Current density up to 3 mA/cm.^{2}.
[d] MeCN analytical reagent quality and electrolyte not dried.
[e] Constant potential electrolysis in a divided cell.
[f] Isolated yield.
[g] In parenthesis is reported the possible current to be applied.

scope of the reaction using MeCN as the solvent and $TBAPF_6$ as the supporting electrolyte in galvanostatic conditions (3.3 mA/cm^2). Concerning the selection of the cathode material for preparative experiments, graphite plate electrodes proved to be highly suitable for preparative cathodic transformations. This suitability arises from their favorable overpotential for the hydrogen evolution reaction (HER) in most organic media. This attractive characteristic, together with their lower cost and greater accessibility in comparison to other electrode materials like platinum, boron-doped diamond (BDD), or nickel, made them the primary factors guiding the choice of the cathode.

The production of **2b** in the cathodic compartment of a divided cell demonstrates that the formation of the carbonyl compound is exclusively a cathodic process, without involving the anode. When THF was used, resistance limitations were observed and it was impossible to achieve the desired current densities (entries 7, 8, and 11), reaching **2b** in moderated yields. The low dielectric constant of THF (8 F/m) in comparison to other solvents such as DMF (37 F/m) and MeCN (38 F/m) was assumed as the reason for this behavior. Nevertheless, when acetonitrile is used as a co-solvent (30 %), the conductivity of the cell is improved and so does the yield of **2a** (entries 13 and 14). Thus, this mixture may be used when a NBOPI is not completely soluble in MeCN, but is in THF, providing alternative conditions to carry out the reaction. Entry 15 was carried out using an analytical reagent quality solvent instead of an anhydrous, without a drying supporting electrolyte, showing that small quantities of water in the electrochemical cell do not inhibit the reaction, but slight erosion of the yield occurs. The yield obtained demonstrated that the reaction is robust despite a small presence of water in the system, indicating that the NBOPI radical anion decomposition to the carbonyl derivative is a very fast reaction, which agrees with the electrochemical response depicted in Fig. 4a. The reactions in general required among 0.8–1.5 F/mol to consume **2a,** which indicates that secondary reactions, besides the mechanism proposed by Terent'ev, are present during the macroelectrolysis. These reactions are not observed in electroanalytical experiments, where theoretically less than 1.0 F/mol of charge would be required to complete the reaction. Thus, the Faradaic efficiency, when considering 1.0 F/mol as the standard amount of charge for this reaction, fluctuates between 125% and 67% for this stage.

The scope and limitations of the described approach were evaluated by applying the selected conditions to NBOPIs bearing redox reactive moieties in either reduction or oxidation (Scheme 5). Fig. 5 presents the CVs of the selected compounds to attain the scope. As the voltammograms show, all substrates presented the characteristic reduction peak in the −1.6 to −1.7 V range corresponding to the NBOPI system's initial reduction. As expected, this cathodic activation triggered the breaking of the *N*–O bond. For **3a**, **5a**, **6a,** and **7a,** the first phthalimide reduction is observed in the CVs of the compounds, at a potential near 1.8 V. Moreover, in all the cases the second phthalimide reduction peak was observed before the cathodic limit (around −3.0 V). For **4a** and **8a**, the number of cathodic peaks does not correspond with the rest of the examples, suggesting that even if the presence of a different functional group may change the cathodic pattern observed, the breaking of the *N*–O bond should occur.

The corresponding carbonyl derivative of the substrates **1a**, **2a**, **7a,** and **8a** was obtained in moderate to good yields using the standard conditions depicted in Scheme 5. **7a** showed the pinacol coupling product from the over-reduction of carbonyl in low yield. Switching the electrolysis to a divided cell, **3b, 5b,** and **6b** are achieved as well, avoiding the anode oxidation of the redox moiety. A remarkable example of the scope of the reaction is the simple access to **5b** and **6b**, which previous reports obtained *via* the hydrogenation of phthalaldehyde catalyzed by palladium in a pressure vessel [40], or using $NaBH_4$ as a reducing agent [41]. The value of this

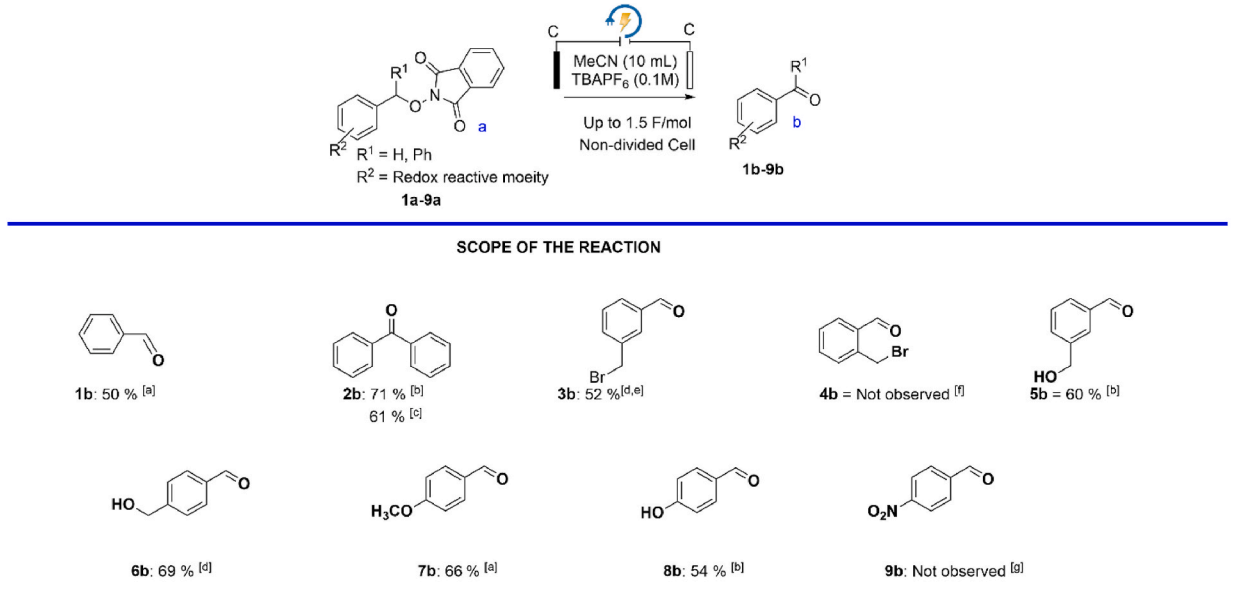

Scheme 5. Scope of the of NBOPIs reduction bearing a redox reactive moiety. [a] Yield determined from the crude reaction using NMR.[2] [b] Isolated yield. [c] Gram scale, synthesis. [d] Isolated yield using a divided cell. [e] 80% of starting material; **3a** recovered using standard conditions. [f] 75% of starting material **4a** recovered using standard conditions. [g] **9a** not recovered.

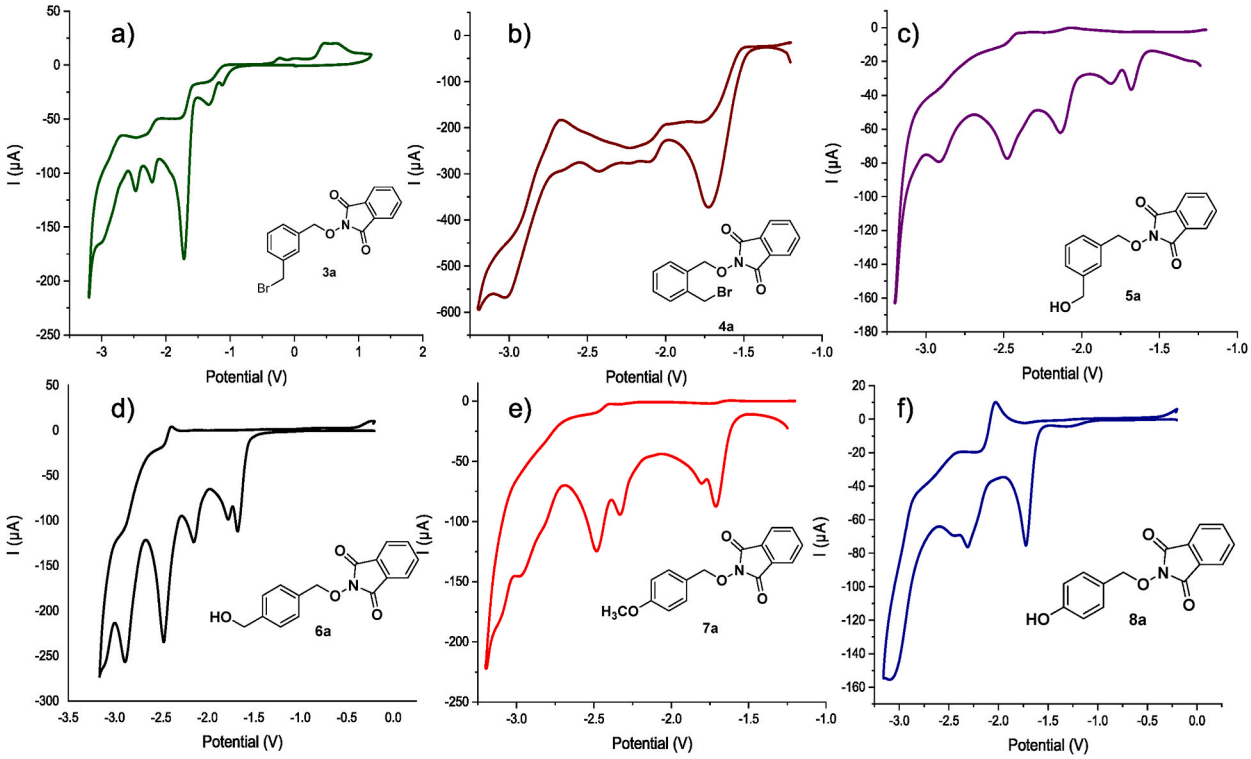

Fig. 5. Cyclic voltammetry of selected NBOPIs: (a) **3a**. (b) **4a**. (c) **5a**. (d) **6a**. (e) **7a**. (f) **8a**. $TBAClO_4$ 0.1 M in DMF, at $\nu = 0.1$ V s^{-1}. WE: Glas sy carbon, CE: Pt, RE: Ag/Ag^{+}.

electrosynthesis may be evaluated by consulting, for example, the commercial price of **5b,** which can be purchased for 3.33 USD/mg, indicating the complexity of its synthesis by other routes [42]. In general, the aldehydes bearing diverse moieties are valuable synthetic intermediates of pharmaceuticals and are generally obtained using two or more reaction steps [[40,41,43–47]]. In most cases, electroreduction of the obtained carbonyl compounds (over-reduction) can be avoided by monitoring the consumption of the initial NBOFI. Since the reduction potential of the NBOFI is sufficiently lower than the produced carbonyl compound, the selective reactivity is feasible as long as the charge applied is well controlled. A gram-scale electrolysis was carried out to prove the synthetic application of the reaction. The electro-reduction of **2a** was easily scaled up to gram quantity in a 61% yield (7.6 mmol scale).

Regarding the challenges of the reaction, benzylic bromides are electrochemical reactive moieties that, in cathodic conditions, trigger the formation of benzylic radicals [23,48,49]. When the electrolysis of **3a** and **4a** was carried out, reduction of the brominated group was the competitive reaction. However, the final product is affected by the type of cell used. When an undivided cell is employed, the reduction of the substrates undergoes the formation of bromide anions, which are oxidized in the anode rendering an orange-colored solution due to the liberation of Br_2. The color disappears when the thiosulfate ion is added, confirming the presence of Br_2 in the solution. Alternatively, the corresponding aldehyde can be isolated when a divided cell is used for the electrolysis of **3a,** but a complex mixture of compounds is produced in the same conditions for **4a** (see supplementary data). The result of the electrolysis of **9a** indicates an incompatibility of the reduction of NBOPIs in the presence of a nitro group, albeit the CV apparently reveals the same pattern observed in the other substrates (see supplementary data). Nevertheless, the carbonyl product is not observed during electrolysis, and the solution turns into a dark color, indicating the competing reduction of the nitro group.

Some control experiments are presented in Scheme 6. Electrolysis of **1a** was conducted in the absence of a power source, and no conversion was observed. Then, the current was alternated on and off for 10 min, but the starting material **1a** was not completely consumed. This indicates that the electrochemical transformation must run continuously with electricity, despite its catalytic nature.

Finally, it was evaluated the reaction's behavior in the presence of a radical trap; TEMPO persistent radical was chosen to demonstrate the existence of free radical intermediates involved in the reaction [50,51]. As expected, after 1.5 F/mol had been passed, most of **1a** was consumed, but no **1b** was observed (Scheme 6, entry c). This result, and the formation of pinacol even when less than 0.5 F/mol of charge had been passed, suggests that the ketyl radical anion (Scheme 3, **KR**) is present in the medium before the aldehyde reduction, confirming its presence, as it was previously suggested.

4. Conclusion

In summary, the access to carbonyl products through the electrochemical reduction of the corresponding *N*-benzyloxyphtalimides obtained from benzylic alcohols was achieved in moderate to good yields (50–71%). The carbonyl compounds are valuable

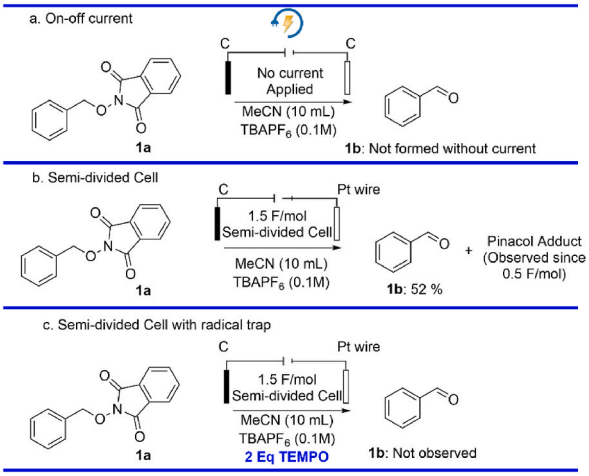

Scheme 6. Control experiments.

intermediates and are usually limited to be accessed through oxidative methods. Our approach can be applied to substrates containing oxidizable moieties, compatible with an electrochemical reductive conditions. Considering that phthalimide is an important byproduct obtained during the electrolysis process, it is necessary to explore its potential recovery and recycling for synthesizing NHPI, as detailed in existing reports [52]. Although the Terent'ev group was the first in reporting this reaction and proposed a putative reaction mechanism [22], the current work explores its synthetic application as a sort of orthogonal oxidizing reaction. Additionally, the proposed mechanism was contrasted and confirmed using simulated and experimental CV, validating that this process is an electrochemical catalyzed reaction.

Data availability statement

The data associated with this study has not been deposited into any publicly available repository but is available in the Supplementary Data. Additional data can be provided upon request.

CRediT authorship contribution statement

Diego Francisco Chicas-Baños: Writing – review & editing, Writing – original draft, Investigation, Formal analysis. **Mariely López-Rivas:** Investigation, Formal analysis. **Felipe J. González-Bravo:** Writing – review & editing, Validation, Software, Investigation, Formal analysis. **Fernando Sartillo-Piscil:** Writing – review & editing, Resources, Project administration, Conceptualization. **Bernardo Antonio Frontana-Uribe:** Writing – review & editing, Supervision, Resources, Project administration, Methodology, Conceptualization.

Declaration of competing interest

The authors declare that they have no known competing financial interests or personal relationships that could have appeared to influence the work reported in this paper.

Acknowledgments

The authors express their gratitude to CONACyT project A1-S-18230 for the financial support granted and for the doctoral scholarship (CVU: 1077008) for the development of this research, to N. Zavala-Segovia, L. Triana-Cruz, A. Nuñez-Pineda, U. Hernández-Balderas, C. Martínez-Soto, J. Pérez-Flores, and M.C. García-González for the technical support provided.

Appendix A. Supplementary data

Supplementary data to this article can be found online at https://doi.org/10.1016/j.heliyon.2023.e23808.

References

[1] R.A. Sheldon, I.W.C.E. Arends, G.-J. ten Brink, A. Dijksman, Green, Catalytic oxidations of alcohols, Acc. Chem. Res. 35 (2002) 774–781, https://doi.org/10.1021/ar010075n.

[2] R.A. Sheldon, Recent advances in green catalytic oxidations of alcohols in aqueous media, Catal. Today 247 (2015) 4–13, https://doi.org/10.1016/j.cattod.2014.08.024.

[3] M. Uyanik, K. Ishihara, Hypervalent iodine-mediated oxidation of alcohols, Chem. Commun. (2009) 2086, https://doi.org/10.1039/b823399c.

[4] Z. Shen, Y. Hu, B. Li, Y. Zou, S. Li, G. Wilma Busser, X. Wang, G. Zhao, M. Muhler, State-of-the-art progress in the selective photo-oxidation of alcohols, J. Energy Chem. 62 (2021) 338–350, https://doi.org/10.1016/j.jechem.2021.03.033.

[5] A.E. Wendlandt, S.S. Stahl, Quinone-catalyzed selective oxidation of organic molecules, Angew. Chem. Int. Ed. 54 (2015) 14638–14658, https://doi.org/10.1002/anie.201505017.

[6] B.A. Frontana-Uribe, R.D. Little, J.G. Ibanez, A. Palma, R. Vasquez-Medrano, Organic electrosynthesis: a promising green methodology in organic chemistry, Green Chem. 12 (2010) 2099–2119, https://doi.org/10.1039/c0gc00382d.

[7] D.F. Chicas-Baños, B.A. Frontana-Uribe, Electrochemical generation and use in organic synthesis of C-, O-, and *N*-centered radicals, Chem. Rec. 21 (2021) 2538–2573, https://doi.org/10.1002/tcr.202100056.

[8] C. Kingston, M.D. Palkowitz, Y. Takahira, J.C. Vantourout, B.K. Peters, Y. Kawamata, P.S. Baran, A survival guide for the "electro-curious,", Acc. Chem. Res. 53 (2020) 72–83, https://doi.org/10.1021/acs.accounts.9b00539.

[9] D. Pollok, S.R. Waldvogel, Electro-organic synthesis-a 21st century technique, Chem. Sci. 11 (2020) 12386–12400, https://doi.org/10.1039/d0sc01848a.

[10] M. Zhang, D. Hu, Y. Chen, Y. Jin, B. Liu, C.H. Lam, K. Yan, Electrocatalytic reductive amination and simultaneous oxidation of biomass-derived 5-hydroxymethylfurfural, Ind. Eng. Chem. Res. 61 (2022) 1912–1919, https://doi.org/10.1021/acs.iecr.1c04508.

[11] S. Kim, T.A. Lee, Y. Song, Facile Generation of alkoxy radicals from *n*-alkoxyphthalimides, Synlett (1998) 471–472, https://doi.org/10.1055/s-1998-1711, 1998.

[12] H. Zhu, J.G. Wickenden, N.E. Campbell, J.C.T. Leung, K.M. Johnson, G.M. Sammis, Construction of carbo- and heterocycles using radical relay cyclizations initiated by alkoxy radicals, Org. Lett. 11 (2009) 2019–2022, https://doi.org/10.1021/ol900481e.

[13] M. Rueda-Becerril, J.C.T. Leung, C.R. Dunbar, G.M. Sammis, Alkoxy radical cyclizations onto silyl enol ethers relative to alkene cyclization, hydrogen atom transfer, and fragmentation reactions, J. Org. Chem. 76 (2011) 7720–7729, https://doi.org/10.1021/jo200992m.

[14] H. Zhu, J.C.T. Leung, G.M. Sammis, Strategies to control alkoxy radical-initiated relay cyclizations for the synthesis of oxygenated tetrahydrofuran motifs, J. Org. Chem. 80 (2015) 965–979, https://doi.org/10.1021/jo502499a.

[15] M. Zlotorzynska, H. Zhai, G.M. Sammis, Chemoselective oxygen-centered radical cyclizations onto silyl enol ethers, Org. Lett. 10 (2008) 5083–5086, https://doi.org/10.1021/ol802142k.

[16] F. Sartillo-Piscil, M. Vargas, C. Anaya De Parrodi, L. Quintero, Diastereoselective synthesis of 1,2-O-isopropylidene-1,6-dioxaspiro[4,4]nonane applying the methodology of generation of radical cations under non-oxidizing conditions, Tetrahedron Lett. 44 (2003) 3919–3921, https://doi.org/10.1016/S0040-4039(03)00817-7.

[17] O. Cortezano-Arellano, L. Quintero, F. Sartillo-Piscil, Total synthesis of cephalosporolide E via a tandem radical/polar crossover reaction. The use of the radical cations under nonoxidative conditions in total synthesis, J. Org. Chem. 80 (2015) 2601–2608, https://doi.org/10.1021/jo502757c.

[18] C.G. Francisco, A.J. Herrera, A.R. Kennedy, A. Martín, D. Melián, I. Pérez-Martín, L.M. Quintanal, E. Suárez, Intramolecular 1,8-hydrogen-atom transfer reactions in (1→4)-*O*- disaccharide systems: conformational and stereochemical requirements, Chem. Eur J. 14 (2008) 10369–10381, https://doi.org/10.1002/chem.200801414.

[19] E.I. León, A. Martín, I. Pérez-Martín, E. Suárez, Reductive Radical cascades triggered by alkoxyl radicals in the β-cyclodextrin framework, Org. Lett. 20 (2018) 3385–3389, https://doi.org/10.1021/acs.orglett.8b01308.

[20] Á. Martín, I. Pérez-Martín, L.M. Quintanal, E. Suárez, Intramolecular 1,8-hydrogen atom transfer. Stereoselectivity of the hexopyranos-5′-yl radical reactions in H*exp*-(1→4)-H*exp* disaccharide systems, J. Org. Chem. 73 (2008) 7710–7720, https://doi.org/10.1021/jo801499d.

[21] M. Zlotorzynska, G.M. Sammis, Photoinduced electron-transfer-promoted redox fragmentation of *N*-alkoxyphthalimides, Org. Lett. 13 (2011) 6264–6267, https://doi.org/10.1021/ol202740w.

[22] M.A. Syroeshkin, I.B. Krylov, A.M. Hughes, I.V. Alabugin, D.V. Nasybullina, M.Y. Sharipov, V.P. Gultyai, A.O. Terent'ev, Electrochemical behavior of *N*-oxyphthalimides: cascades initiating self-sustaining catalytic reductive N–O bond cleavage, J. Phys. Org. Chem. 30 (2017) 1–15, https://doi.org/10.1002/poc.3744.

[23] O. Hammerich, B. Speiser, Organic Electrochemistry, 5th Edition: Revised and Expanded, fifth ed., CRC Press, 2015 https://doi.org/10.1201/b19122.

[24] S.X. Wang, X.W. Li, J.T. Li, Synthesis of *N*-alkoxyphthalimides under ultrasound irradiation, Ultrason. Sonochem. 15 (2008) 33–36, https://doi.org/10.1016/j.ultsonch.2007.07.005.

[25] K.M.K, E.K.R. Jae Nyoung Kim, Improved synthesis of *N*- alkoxyphthalimdes, Synth. Commun. 22 (1992) 1427–1432, https://doi.org/10.1080/00397919308020392.

[26] D.L. Hughes, The Mitsunobu reaction, Org. React. (1992) 335–656, https://doi.org/10.1002/0471264180.OR042.02.

[27] C. Yoshida, K. Tanaka, Y. Todo, R. Hattori, Y. Fukuoka, M. Komatsu, I. Saikawa, Studies on monocyclic β-lactam antibiotics IV. Synthesis and antibacterial activity of (3*S*, 4*R*)-3-[2-(2-aminothiazol-4-yl)-(*Z*)-2-(*O*-substituted oxyimino)acetamido]-4-methyl-1-(1*H*-tetrazol-5-yl)-2-azetidinones, J. Antibiot. 39 (1986), https://doi.org/10.7164/antibiotics.39.90, 90–100.

[28] Y. Lv, K. Sun, T. Wang, G. Li, W. Pu, N. Chai, H. Shen, Y. Wu, NBu4NI-catalyzed intermolecular *C-O* cross-coupling reactions: synthesis of alkyloxyamines, RSC Adv. 5 (2015) 72142–72145, https://doi.org/10.1039/c5ra12691f.

[29] L. Dian, S. Wang, D. Zhang-Negrerie, Y. Du, Organocatalytic Radical involved oxidative cross-coupling of *N*-Hydroxyphthalimide with benzylic and allylic hydrocarbons, Adv. Synth. Catal. 357 (2015) 3836–3842, https://doi.org/10.1002/adsc.201500623.

[30] A. Bartovic, P. Netchitaïlo, A. Daïch, B. Decroix, A facile fused-dioxaza-ring synthesis from *N*-hydroxyphthalimide, Tetrahedron Lett. 40 (1999) 2117–2120, https://doi.org/10.1016/S0040-4039(99)00144-6.

[31] A.O. Terent'ev, I.B. Krylov, M.Y. Sharipov, Z.M. Kazanskaya, G.I. Nikishin, Generation and cross-coupling of benzyl and phthalimide-*N*-oxyl radicals in a cerium (IV) ammonium nitrate/*N*-hydroxyphthalimide/$ArCH_2R$ system, Tetrahedron 68 (2012) 10263–10271, https://doi.org/10.1016/j.tet.2012.10.018.

[32] M.-Z. Wang, H. Xu, T.-W. Liu, Q. Feng, S.-J. Yu, S.-H. Wang, Z.-M. Li, Design, Synthesis and Antifungal Activities of Novel Pyrrole Alkaloid Analogs, 2011, https://doi.org/10.1016/j.ejmech.2011.01.031.

[33] X. Wang, R. Liu, Y. Jin, X. Liang, TEMPO/HCl/$NaNO_2$ Catalyst: a transition-metal-free approach to efficient aerobic oxidation of alcohols to aldehydes and ketones under mild conditions, Chem. Eur J. 14 (2008) 2679–2685, https://doi.org/10.1002/chem.200701818.

[34] A. Tuley, Y.J. Lee, B. Wu, Z.U. Wang, W.R. Liu, A genetically encoded aldehyde for rapid protein labelling, Chem. Commun. 50 (2014) 7424–7426, https://doi.org/10.1039/C4CC02000F.

[35] V.P. Baillargeon, J.K. Stille, Palladium-catalyzed formylation of organic halides with carbon monoxide and tin hydride, J. Am. Chem. Soc. 108 (1986) 452–461, https://doi.org/10.1021/ja00263a015.

[36] I. Mandal, A.F.M. Kilbinger, Practical Route for Catalytic Ring-Opening Metathesis Polymerization, 2022, https://doi.org/10.1021/jacsau.2c00566.

[37] U.K. Warghane, R.P. Dhankar, Novel biosynthesis of silver nanoparticles for catalytic oxidation of Alcohols containing aromatic ring, Mater. Today Proc. 15 (2019) 526–535, https://doi.org/10.1016/j.matpr.2019.04.117.

[38] A. Matzeit, H.J. Schäfer, C. Amatore, Radical Tandem Cyclizations by Anodic Decarboxylation of Carboxylic Acids, Stuttg), Synthesis, 1995, pp. 1432–1444, https://doi.org/10.1055/s-1995-4112, 1995.

[39] R. Francke, R.D. Little, Electrons and holes as catalysts in organic electrosynthesis, Chemelectrochem (2019), https://doi.org/10.1002/CELC.201900432.

[40] A.P. Dunlop, E. Sherman, J.P. Wuskell, United States Patent Office (1974), 3845138.

[41] K. Tong, R. Zhang, F. Ren, T. Zhang, J. He, J. Cheng, Z. Yu, F. Ren, Y. Zhang, W. Shi, Synthesis and evaluation of novel α-aminoamides containing benzoheterocyclic moiety for the treatment of pain, Molecules 26 (2021) 1–14, https://doi.org/10.3390/molecules26061716.
[42] Merck, 3-(Hydroxymethyl)benzaldehyde AldrichCPR 939760-33-5, (n.d.). https://www.sigmaaldrich.com/MX/es/product/aldrich/ph017016. (Accessed 28 May 2023).
[43] N. Aljaar, J. Conrad, U. Beifuss, Synthesis of 2-aryl-1,2-dihydrophthalazines via reaction of 2-(bromomethyl)benzaldehydes with arylhydrazines, J. Org. Chem. 78 (2013) 1045–1053, https://doi.org/10.1021/jo302491x.
[44] L. Dai, S. Ye, NHC-catalyzed ϵ-umpolung via *p*-quinodimethanes and its nucleophilic addition to ketones, ACS Catal. 10 (2020) 994–998, https://doi.org/10.1021/acscatal.9b04409.
[45] D. Janssen-Müller, S. Singha, T. Olyschläger, C.G. Daniliuc, F. Glorius, Annulation of o -quinodimethanes through *N*-heterocyclic carbene catalysis for the synthesis of 1-isochromanones, Org. Lett. 18 (2016) 4444–4447, https://doi.org/10.1021/acs.orglett.6b02335.
[46] G. Xu, Z. Wang, Y. Shao, J. Sun, Copper-catalyzed tandem cross-coupling and alkynylogous aldol reaction: access to chiral exocyclic α-allenols, Org. Lett. 23 (2021) 5175–5179, https://doi.org/10.1021/acs.orglett.1c01712.
[47] M. Li, L.P. Cheng, W. Pang, Z.J. Zhong, L.L. Guo, Design, synthesis, and biological evaluation of novel acylhydrazone derivatives as potent neuraminidase inhibitors, ACS Med. Chem. Lett. 11 (2020) 1745–1750, https://doi.org/10.1021/acsmedchemlett.0c00313.
[48] A.J. Fry, J.M. Porter, P.F. Fry, Electrochemical formation and dimerization of α - substituted benzyl radicals. steric effects on dimerization, J. Org. Chem. 61 (1996) 3191–3194, https://doi.org/10.1021/jo951577f.
[49] D. Vasudevan, Direct and indirect electrochemical reduction of organic halides in aprotic media, Russ. J. Electrochem. 41 (2005) 310–314, https://doi.org/10.1007/S11175-005-0067-2, 2005 413.
[50] C. Wang, Y. Yu, W.L. Liu, W.L. Duan, site-tunable $C sp^{3}$-H bonds functionalization by visible-light-induced radical translocation of *N*-alkoxyphthalimides, Org. Lett. 21 (2019) 9147–9152, https://doi.org/10.1021/acs.orglett.9b03524.
[51] L.L. Chai, Y.H. Zhao, D.J. Young, X. Lu, H.X. Li, Ni(II)-Mediated photochemical oxidative esterification of aldehydes with phenols, Org. Lett. 24 (2022) 6908–6913, https://doi.org/10.1021/acs.orglett.2c02560.
[52] C. Einhorn, J. Einhorn, C. Marcadal-Abbadi, Mild and convenient one pot synthesis of *N*-hydroxyimides from n-unsubstituted imides, Synth. Commun. 31 (2001) 741–748, https://doi.org/10.1081/SCC-100103264.